



HAL
open science

Preliminary Co-Design of L and X-band Stacked Arrays with Scanning Capabilities

Brandon Sun, Renaud Loison, Raphaël Gillard, Eric Estebe, Christian Renard

► **To cite this version:**

Brandon Sun, Renaud Loison, Raphaël Gillard, Eric Estebe, Christian Renard. Preliminary Co-Design of L and X-band Stacked Arrays with Scanning Capabilities. EuCAP 2020, Mar 2020, Copenhagen, Denmark. hal-02794561

HAL Id: hal-02794561

<https://hal.science/hal-02794561>

Submitted on 5 Jun 2020

HAL is a multi-disciplinary open access archive for the deposit and dissemination of scientific research documents, whether they are published or not. The documents may come from teaching and research institutions in France or abroad, or from public or private research centers.

L'archive ouverte pluridisciplinaire **HAL**, est destinée au dépôt et à la diffusion de documents scientifiques de niveau recherche, publiés ou non, émanant des établissements d'enseignement et de recherche français ou étrangers, des laboratoires publics ou privés.

Preliminary Co-Design of L and X-band Stacked Arrays with Scanning Capabilities

Brandon Sun^{1,2}, Renaud Loison¹, Raphaël Gillard¹, Éric Estebe², Christian Renard²

¹Institut d'Électronique et de Télécommunications de Rennes, INSA Rennes, France, brandon.sun@insa-rennes.fr

²Thales Defense Mission Systems, Élancourt, France

Abstract—The design of L and X-band stacked arrays is presented in this paper. The design of the X-band element is first detailed. The use of stacked patches leads to scan angles up to 60° in E-plane, and 54° in H-plane, in the 9.5-10.5 GHz band (active reflection coefficient < -10 dB). Secondly, the design of the L-band source is presented. The use of stacked dipoles results in scan angles up to 60° in the H-plane, for the two Identification Friend or Foe (IFF) bands, at 1.03 and 1.09 GHz (with 3.6 MHz bandwidths). Finally, the L-band dipoles are placed above the X-band array and the performances of the stacked arrays are analyzed in the L and X-bands.

Index Terms—antenna, phased arrays, dual-band, wide angle scanning

I. INTRODUCTION

Due to the restricted volume for their implementation, the integration of multifunctional antenna systems (radar, telecommunication, identification, etc.) on carrier devices (satellites, ships or planes) is becoming more and more difficult. The growing number and complexity of these systems reinforce this issue. In this context, accommodating two independent phased arrays on the same surface is an attractive solution to save space.

In this paper, an L/X dual-band antenna system is investigated. A dual linear polarization is required in the X-band while a single linear polarization is needed in the L-band for IFF (Identification Friend or Foe) application. Relative wide bandwidths and wide scanning capabilities are needed for the two bands as presented in Table I. The center frequencies are 10 GHz for X-band and the two IFF frequencies, 1.03 and 1.09 GHz, for L-band. The two arrays must be fully independent and thus must have their own excitations.

In [1] and [2], the concept of perforated dual-band dual-polarized (DBDP) microstrip patch array is presented. In both cases, the proposed solutions are unsuitable for our application due to very limited scanning capabilities and narrow bandwidths. Furthermore, the frequency ratio is less than 1:4, which is too low for our application. The required frequency ratio of about 1:10 prohibits the use of sandwich-stacked patches as in [3] where the lower-band element is placed below the higher-band one. Moreover, even if these structures offer relative wide bandwidths, they are not adapted due to the complexity of the excitation. A dual-band array system providing a frequency ratio of 12 is presented in [4]. An X-band microstrip patch array is integrated into a

superstrate layer covering printed dual-band slot loop antennas. The slot loop antennas resonate at 1 GHz (for the larger one) and 2 GHz (for the smaller one), which are two relative distant frequencies compared to the two IFF frequencies we have to deal with. It seems difficult to design separate slot loop antennas with resonance frequencies as close as expected in our work.

In this paper, an antenna system made of two superimposed arrays designed for L and X-bands is presented. Due to the relative wide expected bandwidths, stacked patches are used for the X-band and stacked dipoles for the L-band. The dipoles are located above the patches.

The paper is organized as follows. First, in Section II, the X-band and L-band structures are presented. In Section III, the potential dual-band array is introduced and the performance is analyzed. Finally, in Section IV, the conclusions are exposed.

II. SEPARATE DESIGN OF THE X-BAND AND L-BAND ARRAYS

A. X-band

The X-band element must operate in dual linear polarization with a center frequency equal to 10 GHz and a 1 GHz bandwidth (10 %). Nonetheless, a single linear polarization is considered in this preliminary work for the sake of simplicity. Beam scanning up to 60° in both principal planes is required for the targeted application. Fig. 1a and 1b depict the proposed structure. It consists of two stacked square patches printed on low-loss dielectric layers ($\epsilon_r = 3.41$, $\tan\delta = 0.002$). A thick air layer separating the two patches aims at enlarging the bandwidth. A metallic cavity is used to limit mutual coupling. Its horizontal extension as a grid on the top substrate (controlled by gap g) also provides an additional parameter to tune the performance. Individual coaxial feeds are used for each element in the array.

The spacing between radiating elements is set to 14 mm, which is lower than half the wavelength at the upper frequency. Dielectric thicknesses ($h_1 = 0.81$ mm and $h_3 = 0.51$ mm) are chosen from available standard values. The structure is then optimized from extensive parametric studies with Ansoft HFSS. The five variable parameters are the dimensions of the square patches (L_1 and L_2), the height of the air layer (h_2), the position of the coaxial probe on the driven patch (p_1), and finally, the distance between the grid

TABLE I. DESIGN SPECIFICATIONS

Parameters	L-band	X-band
Frequency	1.03 and 1.09 GHz	10 GHz
Considered bandwidth	6 MHz around each frequency	1 GHz
Scan range	$\pm 60^\circ$ in the H-plane	$\pm 60^\circ$ in the two principal planes
Polarization	Vertical	Dual linear

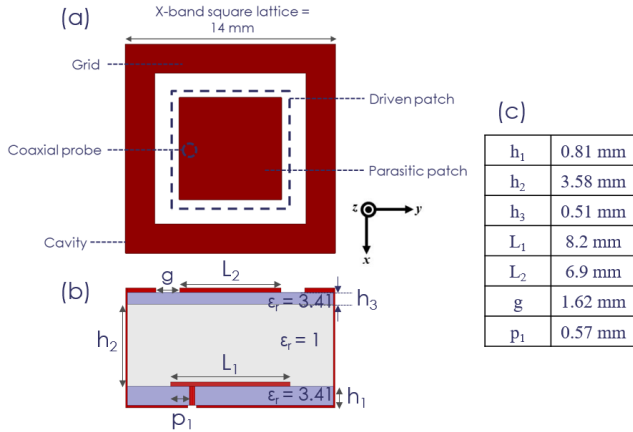


Fig. 1 (a) Top and (b) side views of a unit cell of the X-band array, (c) main characteristics

and the parasitic patch (g). The optimized values are given in Fig. 1c. All simulations are realized using master-slave periodic boundary conditions along the x and y-directions to mimic an infinite periodic environment.

Fig. 2 shows the active reflection coefficient for different scanning angles in the E and H-planes. The -10 dB bandwidth is 1 GHz. A scan up to 60° is achieved in the E-

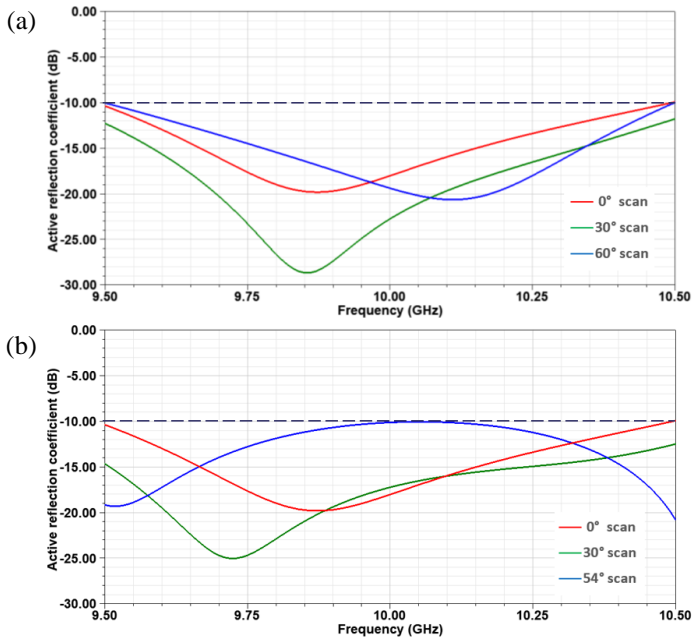


Fig. 2 Simulated active reflection coefficients, for X-band, versus frequency for different scan angles and planes, (a) E-plane, (b) H-plane.

plane. However, the scanning capability in the H-plane is limited to 54° .

B. L-band

The L-band element must operate in vertical polarization at the two IFF frequencies, 1.03 and 1.09 GHz. Beam scanning up to 60° in the H-plane is required for the targeted identification application. Fig. 3a and 3b illustrate the proposed structure.

It is obtained by adding two air layers on top of the X-band stack-up. Each of them supports an L-band dipole. At this stage, the optimization of the L-band stack-up is carried out without accounting for all X-band elements. For the sake of realism, only the two X-band elements surrounding the L-band excitation probe, in the y-direction, are considered in the simulation. A ground plane replaces all other X-band elements. A hole is dug in the ground plane to accommodate the central core of the coaxial excitation. A hexagonal lattice is chosen to place the dipoles without overlapping in the x-direction. Parameter c, representing the length of the hexagon side, is set to 97 mm in order to prevent from grating lobes. A capacitive loading is used at the center of the dipoles to improve their matching. It is done by widening the dipoles locally. Finally, there are eleven variable parameters to optimize the L-band structure: the dimensions of the dipoles (w_3, L_3, w_4, L_4), the four dimensions of the widening in the center of the dipoles (not specified here), the position of the coaxial probe on the driven dipole (p_3), and the heights of air layers (h_4, h_5). Their final values are given in Fig. 3c. Simulations are carried out for a single hexagonal cell assuming periodic boundary conditions.

Fig. 4 shows the active reflection coefficient for different scanning angles in the H-plane. A scan up to 50° is obtained

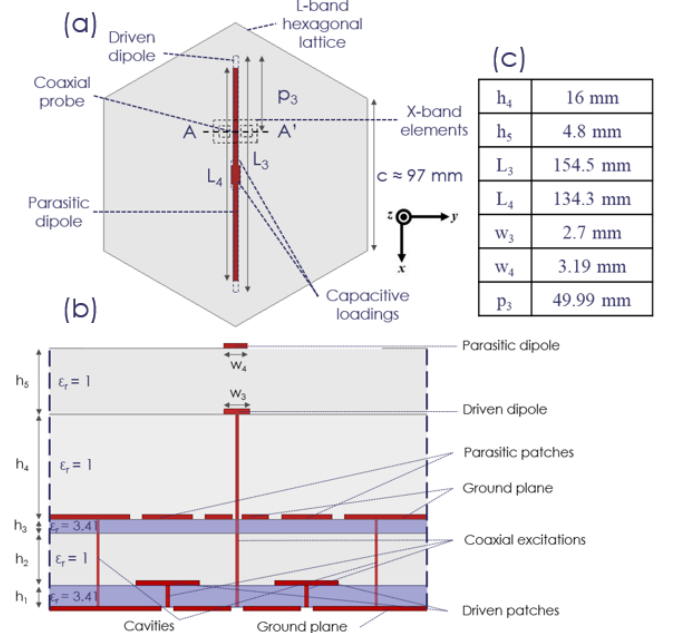


Fig. 3 (a) Top view of a unit cell of the L-band array, (b) side view ([AA'] cut) of the central part of the cell, (c) main characteristics

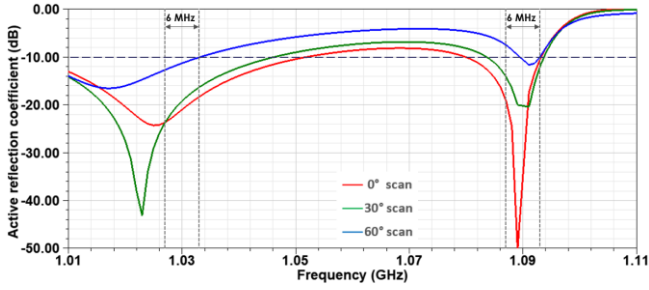


Fig. 4 Simulated active reflection coefficients, for L-band, with frequency for different angles of incidence in H-plane

in the H-plane for the two IFF bands, for a -10 dB bandwidth of 6 MHz. When scanning at 60° , the bandwidth is reduced to 3.6 MHz at the higher IFF frequency (1.09 GHz).

At this stage, no further optimization was done before both arrays are combined together, as presented in the next section.

III. DUAL-BAND ARRAY

A. Effects of the X-band array on the L-band array

In order to study the effects of the X-band array on the L-band array, the X-band elements are now introduced, as shown in Fig. 6. As can be seen in Fig. 5, 12 X-band elements can be accommodated along y in the center row of the L-band hexagonal cell. For the sake of simplicity, truncated patches (see Fig. 5) are suppressed in the simulation. There are then 104 X-band elements in each L-band cell. Simulations are carried out for a single hexagonal cell assuming periodic boundary conditions.

Fig. 7 shows the active reflection coefficient for different scanning angles in the H-plane. The addition of the X-band elements below the dipoles results in a slight shift downwards for the L-band resonant frequencies, especially for the lower one. For a -10 dB bandwidth equal to 6 MHz for the two IFF bands, a scan from 14° to 47° is obtained.

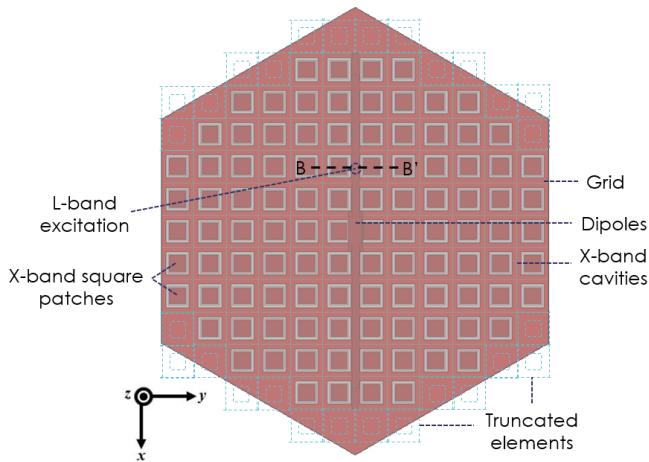


Fig. 5 Layout (showing only metallic elements) of a hexagonal unit cell simulated to analyze X-band elements effects on the L-band array

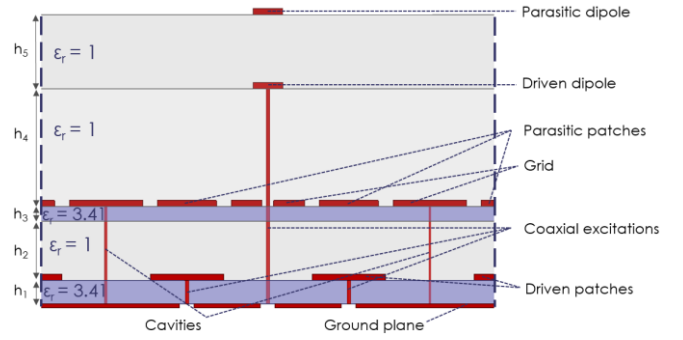


Fig. 6 Side view ([BB'] cut) of the central part of the hexagonal cell

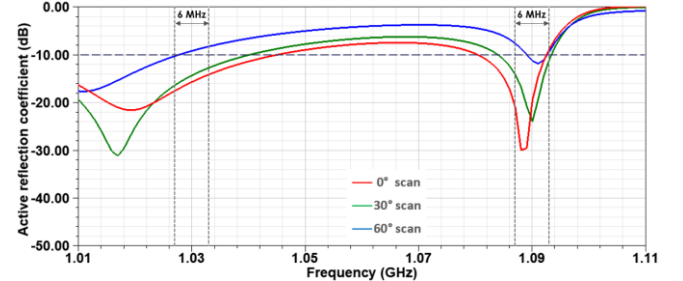


Fig. 7 Simulated active reflection coefficients, for L-band, versus frequency for the different angles of incidence in H-plane, in the presence of the X-band elements

The -10 dB bandwidth is less than 6 MHz for scan from 0° to 13° for the upper IFF frequency, and from 48° to 60° for the lower and/or upper IFF frequencies.

A re-optimization will be necessary with the X-band elements below the dipoles to readjust the resonance frequencies and to achieve the expected performances.

B. Effects of the L-band array on the X-band array

The simulation of a complete hexagonal cell at X-band frequencies requires too much time and memory storage. In order to assess the impact of L-band dipoles on the performance of the X-band array, only the central row, composed of 12 X-band elements, is simulated as seen in Fig. 8. Periodic boundary conditions are used, which means the dipoles are now replaced by infinite strips (free of any excitation and capacitive loading). The widths of the two stacked strips are those of the two dipoles (w_3 and w_4).

The effects on the active reflection coefficients are shown in Fig. 9, for the case where the array radiates at broadside.

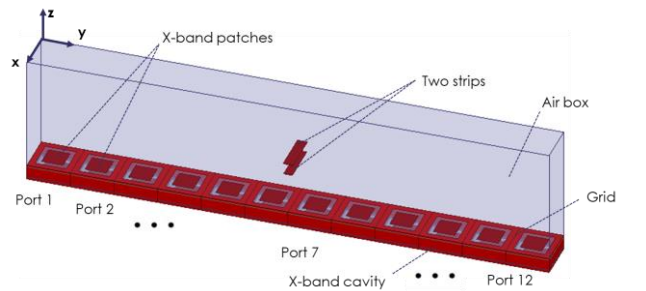


Fig. 8 Topology of the linear array simulated to analyze the L-band effects on the X-band elements according to their position in the array

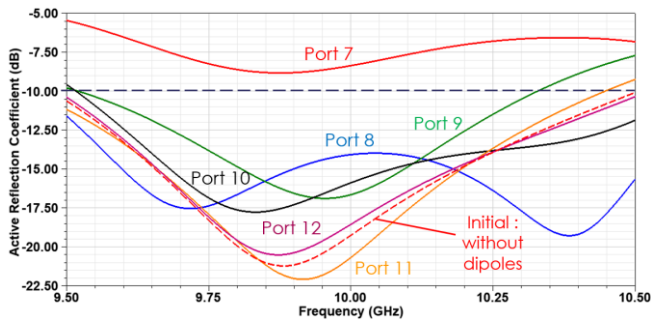


Fig. 9 Influence of the two strips on the active reflection coefficients of X-band elements depending on their position in the array, at broadside

The ports being symmetrical to the dipoles, it is only necessary to study half of them. Globally, the L-band dipoles are responsible for deterioration in the X-band matching. The central patch (port #7) is affected on the whole bandwidth. Port 8 is also significantly disturbed but its matching is preserved. For more distant patches, the perturbation gets rapidly much lower: a relative good matching is preserved in most of the band for ports 9 to 10 and even in the whole band for 11 and 12. Similar behavior (not shown) is observed for other angles of incidence.

As expected, the maximum realized gain is greater when the angle of scanning is lower, as presented in Fig. 10. Indeed, gain losses, due to the two strips, vary between 0.36 and 0.44 dB at broadside, between 0.43 and 0.48 dB for a 30° scan, and between 0.73 and 0.88 dB for a 60° scan.

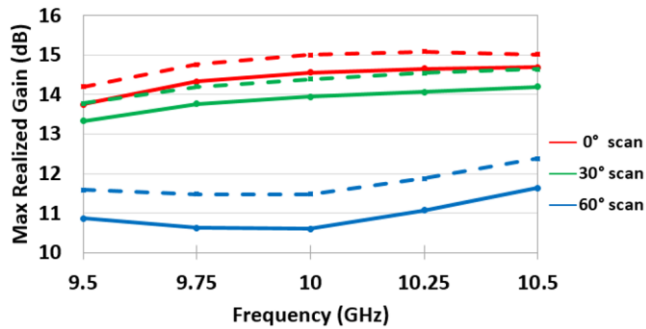


Fig. 10 Evolution of the maximum realized gain versus frequency for different scan angles in the H-plane, without the strips (dotted lines) and with the strips (solid lines)

CONCLUSION

This paper deals with the implementation of an L/X dual-band array on a single shared aperture. First of all, the L-band and X-band arrays have been designed separately. The optimized structures and simulated results are presented. The combination of the two arrays on the same structure is introduced. The effects of one upon the other are analyzed. For both arrays, the scanning range is reduced and the matching is partially degraded. A further optimization would be needed to perfectly meet the specifications.

REFERENCES

- [1] D.M. Pozar and S.D. Targonski, "A shared-aperture dual-band dual-polarized microstrip array," *IEEE Trans. Antennas Propagat.*, Vol. 49, no. 2, 150–157, 2001.
- [2] L.L. Shafai, W.A. Chamma, M. Barakat, P.C. Strickland, and G. Seguin, "Dual-band dual-polarized perforated microstrip antennas for SAR applications," *IEEE Trans. Antennas Propagat.*, Vol. 48, No. 1, 58–66, 2000.
- [3] Z. Sun, K.P. Esselle, S.S. Zhong, and Y.J. Guo, "Shared-aperture dual-band dual-polarization array using sandwiched stacked patch," *Progress In Electromagnetics Research C*, Vol. 52, 183-195, 2014.
- W. Hunsicker, K. Naishadham and R. Hasse, "Integration of an X-Band Microstrip Patch Array and Beamformer for a Multifunction Antenna Array", *IEEE International Symposium on Phased Array Systems and Technology*, 2010.